International Journal of Nanomedicine

Dovepress
Taylor & Francis Group

Open Access Full Text Article

ORIGINAL RESEARCH

PEG-NH_2-Modified Gold Nanoparticle Deliver miRNA-140 for Effective Treatment of Osteoarthritis

Xiangping Luo, Xiaochun Jiang, Zheng Kang

Department of Orthopaedics, Affiliated Hengyang Hospital of Hunan Normal University & Hengyang Central Hospital, Hengyang, Hunan, 421001, People's Republic of China

Correspondence: Xiangping Luo; Zheng Kang, Department of Orthopaedics, Affiliated Hengyang Hospital of Hunan Normal University & Hengyang Central Hospital, Hengyang, Hunan, 421001, People's Republic of China, Tel +86-13974732005, Fax +86-0734-8675740, Email luoxiangping@hunnu.edu.cn; zhengkang@hunnu.edu.cn

Background: Osteoarthritis is a prevalent disease that causes pain and disability in older adults. MicroRNA-140 (miR-140) emerges as a promising therapeutic agent as it suppresses cartilage-degrading enzymes (eg, ADAMTS5, MMPs). However, its clinical translation is limited by rapid intra-articular degradation and poor chondrocyte penetration. The purpose of this experiment was to construct a nanocarrier for delivering miR-140 into chondrocytes, and to detect its delivery efficiency and biological effects.

Methods: We engineered polyethylene glycol-aminated gold nanoparticles (AuNPs-PEG-NH_2) for miR-140 delivery. The efficiency of AuNPs-PEG-NH_2-mediated miR-140-5p (AuNPs-miR-140) delivery was assessed by fluorescence microscopy and flow cytometry. The biological function of AuNPs-miR-140 complexes was detected by quantitative real-time polymerase chain reaction (RT-qPCR), Western blot, and enzyme-linked immunosorbent assay. The effect of AuNPs-miR-140 in attenuating osteoarthritis progression was tested in a mouse model.

Results: Fluorescence microscopy and flow cytometry revealed efficient delivery of miR-140-5p into ATDC5 cells by AuNPs-PEG-NH_2. RT-qPCR analysis demonstrated a controlled sustained release of miR-140-5p from the nanocarriers, maintaining elevated miR-140-5p levels for 14 days. In vitro, AuNPs-miR-140 significantly suppressed catabolic factors (MMP-13 and ADAMTS5; $p<0.01$) and upregulated anabolic markers (COL2 and ACAN; $p<0.01$) in IL-1β-stimulated chondrocytes. Consistent with these findings, in vivo studies showed that AuNPs-miR-140 significantly attenuated cartilage degradation in mice with osteoarthritis, and preserved cartilage structural integrity.

Conclusion: AuNPs-PEG-NH_2 is an efficient intra-articular miRNA delivery platform that successfully overcame the critical limitations of free miRNA therapy. This system effectively restored cartilage homeostasis and delayed osteoarthritis progression by prolonging miR-140 bioactivity and promoting chondrocyte uptake.

Keywords: cartilage, gold nanoparticles, microRNA, osteoarthritis

Introduction

Osteoarthritis (OA) is a common chronic joint disease, particularly prevalent in older adults. The disease is characterized by joint pain and dysfunction and is an important cause of disability.[1] The pathophysiological mechanisms of OA involve complex interactions between mechanical, inflammatory, and genetic factors.[2] Studies have shown that inflammatory mediators and matrix metalloproteinases (MMPs) are key drivers of disease progression, as they promote cartilage degradation and trigger pain. Current therapeutic strategies focus on symptom management (eg, analgesic therapy) but fail to stop or reverse cartilage degeneration. Notably, strategies for slowing cartilage degeneration and repairing damaged cartilage still face significant challenges.[3]

https://doi.org/10.2147/IJN.S585900
Received: 2 December 2025
Accepted: 15 June 2026
Published: 23 June 2026

Gene therapy is a promising direction in OA treatment, as it could alter disease progression by targeting specific molecular pathways in OA pathogenesis. The core strategy is to modulate gene expression or correct genetic defects by delivering nucleic acids, thus providing patients with OA-targeted and potentially curative treatment options.[4,5]

MicroRNA-140 (miR-140) is a crucial regulator that maintains cartilage homeostasis and inhibits cartilage degeneration, particularly in OA. miR-140 is specifically expressed in cartilage tissues and significantly inhibits OA progression by targeting and regulating cartilage degradation and inflammation-related molecular pathways. Studies have shown that miR-140 effectively inhibits the expression of cartilage matrix-degrading enzymes such as ADAMTS5 and MMPs—the main drivers of cartilage destruction in OA.[6,7] miR-140 maintains the structural integrity of the cartilage matrix by downregulating the activity of these enzymes. Furthermore, miR-140 regulates inflammatory pathways that promote cartilage degeneration, including the nuclear factor κB (NF-κB) signaling pathway, the core regulatory hub of the OA inflammatory response. It also creates a favorable microenvironment for cartilage repair by decreasing pro-inflammatory cytokines and other inflammatory mediators.[8,9] Animal experiments have confirmed that intra-articular injection of miR-140 can significantly delay OA progression, highlighting its therapeutic potential.[7,10]

Although local delivery of exogenous genes can be achieved by intra-articular injection, it is difficult for these genes to fully interact with chondrocytes in the three-dimensional cartilage matrix to exert their regulatory effects.[11] Under inflammatory states such as OA, intra-articular nucleases rapidly degrade exogenous miR-140, severely limiting its therapeutic effect.[12] Therefore, developing efficient and safe exogenous miR-140 delivery vectors is key to realizing its therapeutic value in OA.

Researchers focus on developing diversified delivery platforms to enhance the delivery efficiency of miR-140, including viral vector systems, cationic liposomes, polymeric nanoparticles, exosomes, hydrogel delivery systems, and targeted delivery technologies.[13–17] Although each system has its advantages, continuous research should help overcome technical bottlenecks to realize the clinical translation of miR therapeutics.

Gold nanoparticles (AuNPs) have attracted much attention in nucleic acid delivery due to their easy functionalization, excellent biocompatibility, low immunogenicity, and enhanced cellular uptake.[18,19] The biostability and targeting specificity of AuNPs can be enhanced by surface modification with polyethylene glycol (PEG), polyethyleneimine (PEI), or targeting ligands.[20,21] Precise regulation of physicochemical parameters, such as particle size, surface charge, and ligand density of AuNPs-miRNA complexes, is key to achieving efficient gene regulation and low cytotoxicity.[22]

This study innovatively constructed PEG and amino group (NH_2) dual-modified AuNPs (AuNPs-PEG-NH_2) as a platform for cartilage-targeted miR-140 delivery. The PEG-NH_2 modified layer endowed the nanoparticles with physiological stability and facilitated efficient miR loading due to their positively charged surface. We hypothesized that this delivery system could help arrest OA progression effectively by enhancing miR-140-5p stability, promoting chondrocyte-specific uptake, and synergistically regulating inflammatory and catabolic pathways. To test this hypothesis, we systematically characterized the physicochemical properties of AuNPs-PEG-NH_2, assessed its miR-140-5p loading and release kinetics, and comprehensively evaluated its therapeutic efficacy in in vitro and in vivo OA models.

Materials and Methods

Synthesis and Modification of AuNPs

AuNPs-PEG-NH_2 (R-GPN010005-2k) was synthesized by Xi'an Ruixi Biological Technology Co., Ltd., using the classic citrate-based reduction method.[23] Briefly, 50 mL of 0.01% $HAuCl_4 \cdot 3H_2O$ was heated to boiling, followed by the rapid addition of 0.5 mL of 1% sodium citrate. The solution transitioned from pale yellow to wine-red, indicating AuNP formation. SH-PEG2000-NH_2 (5-fold molar excess relative to AuNP surface sites) was dissolved in ultrapure water by sonication (30 min, 40 kHz), then mixed with the AuNPs, and stirred (200 rpm, 25°C, 24 h) at pH 5.0 ± 0.2 to promote thiol-gold binding. The product was purified by centrifugation (10,000 × *g*, 15 min) and washed twice with ultrapure water (pH 6.5).

Preparation of AuNPs-miR-140 Complexes

AuNPs-PEG-NH_2 freeze-dried powder (500 μg) was dissolved in 2 mL of ultrapure water and vortexed thoroughly for 10 min using a bath sonicator, to obtain a homogeneous suspension (250 μg/mL). The suspension was stored at 4°C until use. miR-140-5p (5 nmol, 2 optical density; 178318, GenePharma, Suzhou, China) was dissolved in 250 μL of nuclease-free ultrapure water to

achieve a 20 μM solution (equivalent to 20 pmol/μL). The solution was stored at –80°C. Thirty minutes before cell treatment, 40 μL of AuNPs suspension (250 μg/mL) was combined with 2 μL of miR-140-5p solution (20 μM) in a sterile microtube, achieving a mass ratio of 17.8:1 (AuNPs:miRNA). The mixture was vortexed vigorously for 30 sec and incubated at room temperature for 30 min to facilitate electrostatic conjugation, to achieve an AuNPs-PEG-NH_2-miR-140-5p (termed AuNPs-miR-140) complex solution. The complexes were diluted with Opti-MEM reduced-serum medium (2508952, Gibco, Carlsbad, CA, USA) to the desired working concentration immediately before adding them to cells. This yielded an AuNPs-miR-140 complex solution that contained 10 μg/mL AuNPs and 40 nM miR-140-5p.

Characterization of AuNPs and AuNPs-PEG-NH_2

The morphology and size of AuNPs and AuNPs-PEG-NH_2 were characterized by field emission transmission electron microscopy (FETEM, JEM-F200, JEOL, Japan). The hydrodynamic diameter and zeta potential were measured by a nanoparticle size potential analyzer (NanoBrook 90 plus PALS, Brookhaven, USA). Electronic vibrations and surface functional groups of AuNPs and AuNPs-PEG-NH_2 were measured by ultraviolet-visible spectroscopy (TU-1810, Persee, Beijing, China).

Chondrocyte Culture and Differentiation

ATDC5 cells (iCell-m084, Shanghai, China) were confirmed to be free of mycoplasma contamination. The cells were cultured as a monolayer at a density of 6000 cells/cm^2 in six-well plates using Dulbecco's Modified Eagle's Medium/Nutrient Mixture F-12 (DMEM/F-12; WH0023N141, Procell, Procell Life Science & Technology Co., Ltd, Wuhan, China) supplemented with 5% fetal bovine serum (FBS; SA231102, Procell) and 1% bovine serum albumin (BSA). For differentiation, the cells were maintained in DMEM/F-12 and GlutaMAX I (1:1), containing 10% FBS, penicillin (100u/mL), streptomycin (100μg/mL) sodium pyruvate (55 mg/L) and 1% selenium. When the cell culture reached confluency after a 6-day incubation, the culture medium was further supplemented with β-glycerophosphate (10 mM) and L-ascorbate-2-phosphate (50 μg/mL). The differentiation process was carried out over two weeks, with the culture medium replaced every two days.

Cells Viability Assay After Transfection with AuNPs-miR-140 Complexes

The ATDC5 cells were seeded in 96-well plates at a density of 1×10^4 cells/well and cultured at 37°C, 5% CO_2, and saturated humidity for 24 hours. The culture medium was changed six hours before transfection. Increasing concentrations of AuNPs-miR-140 complexes (AuNPs: 5–40 μg/mL; miR-140-5p: 10–80 nM) were administered to ATDC5 cells for 48 hours. Subsequently, 10 μL of CCK-8 (LFB23028, Life iLab, Shanghai, China) solution was added to each well, and the cells were incubated for two hours. After the incubation, the absorbance was measured at 450 nm on a microplate reader (Epoch2, BioTek, Winooski, VT, USA).

Transfection and Detection of Cellular Uptake of AuNPs-miR-140 Complexes

Fluorescence microscopy (BX51, Olympus, Tokyo, Japan) and flow cytometry (CytoFLEX S, Beckman Coulter, Brea, CA, USA) were used to observe Cy3-miR-140-5p (Cy3-miR-140, 178318, GenePharma, Suzhou, China) uptake by ATDC5 cells. The AuNPs-miR-140 complex solution was prepared 15 minutes before transfection. During the experiment, ATDC5 cells in the logarithmic growth phase were seeded onto a 12-well plate at a density of 5×10^4 cells per well and incubated at 37°C and 5% CO_2 in an incubator (3111, ThermoFisher Scientific, Waltham, MA, USA) for 24 hours. After replacing the culture medium with serum-free DMEM/F12 medium (WH0023N141, Procell), AuNPs-miR-140 complex solution at various concentrations (AuNPs: 0,5,10 μg/mL; miR-140-5p: 40–80 nM) was added to the wells. After 12 hours, the culture medium was replaced with serum medium.

Lipofectamine™ 3000 Reagent (Lipo 3000, 2563912, ThermoFisher Scientific) was used as positive control, and the transfection of it was carried out following the manufacturer's protocol.

After 24 hours, images of the cells were taken on an inverted fluorescence microscope (Evos, Life, Hillsboro, OR, USA), and the cells were digested with 0.25% trypsin (WHAB23F24, Procell) in preparation for flow cytometry analysis.

Reverse Transcription Quantitative Real-Time Polymerase Chain Reaction (RT-qPCR)

Total RNA was extracted from the ATDC5 cells using the TRIzol reagent (GR2211013, ServiceBio, Wuhan, China) according to the manufacturer's instructions. Reverse transcription was performed using stem-loop primers. The sequences of the primers used in the PCR reaction are displayed in Table 1. A real-time PCR detection system (StepOnePlus, ABI, Shanghai, China) was used to quantify the relative RNA expression of the target genes. U6 was used as the internal reference, and the relative mRNA expression was calculated using the $2^{-\Delta\Delta Ct}$ method.

Release Kinetics of AuNPs-miR-140 Complexes

For the in vitro intracellular miR-140-5p expression analysis, ATDC5 cells were seeded in 6-well plates (5×10^6 cells/well) and treated with AuNPs-miR-140 complexes at a concentration of 10 μg/40 nM. Cells were harvested at 12 and 24 hours, and at 3, 7, and 14 days. Total RNA was extracted using the TRIzol reagent, and the level of miR-140-5p was analyzed by RT-qPCR, as described above. Untreated cells, cells treated with free miR-140-5p, and Lipo-miR-140-5p(Lipo-miR-140)-transfected cells served as controls.

Western Blot

ATDC5 cells were seeded in 12-well plates at a density of 1.0×10^5 cells/well. The cell transfection started after 24 hours, when the cell confluency, observed under the microscope, reached approximately 90%. The culture medium was changed six hours before transfection. The original medium was aspirated, and AuNPs-miR-140, Lipo-miR-140, and free miR-140-5p, diluted in serum-free DMEM/F12 medium, were added to the wells. The serum-free medium was replaced with complete medium six hours after transfection in the Lipo-miR-140 group and 12 hours after transfection in the other groups; subsequently, the cells were incubated for 48 hours.

The total protein was extracted from the ATDC5 cells using radioimmunoprecipitation assay (RIPA) buffer (P0013B, Solarbio, Beijing, China) and phenylmethylsulphonyl fluoride (PMSF; CR2303056, Biyotime, Shanghai, China). Total protein was then quantified using a BCA protein assay kit (020123230530, Biyotime). The proteins in the cell lysates were diluted in a loading buffer (EZ6408AB7C, BioFROXX GmbH, Einhausen, Germany), separated by sodium dodecyl sulfate polyacrylamide gel electrophoresis (SDS-PAGE), transferred to a nitrocellulose membrane (75936355, Pall, Port Washington, NY, USA), and blocked in 5% skim milk. The membranes were incubated overnight at 4°C with primary antibodies against MMP-13 (1:1000; 00061706, Proteintech, Wuhan, Hubei, China), ADAMTS5 (1:500; 2f41030, Affinity, Jiangsu, China),

Table 1 Sequence of Primers Used in RT-qPCR Analysis to Detect mRNA Expression

Name	Primer	Sequence (5'-3')
MMP13	Forward	TGTTTGCAGAGCACTACTTGAA
	Reverse	CAGTCACCTCTAAGCCAAAGAAA
ADAMTS5	Forward	CCCAGGATAAAACCAGGCAG
	Reverse	CGGCCAAGGGTTGTAAATGG
COL2	Forward	GGGTCACAGAGGTTACCCAG
	Reverse	ACCAGGGGAACCACTCTCAC
ACAN	Forward	AGGTGTCGCTCCCCAACTAT
	Reverse	CTTCACAGCGGTAGATCCCAG
miR-140-5P	Forward	CGCGCGCGCAGGGACC
	Reverse	AGTGCAGGGTCCGAGGTATT
U6	Forward	GCTTCGGCAGCACATATACTAAAAT
	Reverse	CGCTTCACGAATTTGCGTGTCAT
ACTB	Forward	GGCTGTATTCCCCTCCATCG
	Reverse	CCAGTTGGTAACAATGCCATGT

Abbreviations: ACAN, Aggrecan; ADAMTS5, a disintegrin and metalloproteinase with thrombospondin motifs 5; COL2, collagen 2a1; MMP13, matrix metalloproteinase-13; ACTB, β-Actin.

Aggrecan (ACAN; 1:1000; 00139508, Proteintech), collagen II (COL2; 1:1000; H651466038, HuaBio, Hangzhou, China), and β-actin (1:20,000; 10027685, Proteintech). Subsequently, they were incubated for one hour at room temperature with horseradish peroxidase (HRP)-conjugated sheep anti-mouse/rabbit secondary antibodies (1:5000; 20,001,101/20001329, Proteintech). The membranes were washed four times for five minutes each with Tris-buffered saline Tween 20 (TBST) solution. Electrochemiluminescence (242618E01-02, UElandy, Suzhou, China) solution was added, and the membranes were placed in an imaging device (ChemiDoc XRS+, Bio-Rad, Hercules, CA, USA) for the chemiluminescence reaction. The relative intensities of the blots were quantified by ImageJ software (version 1.51J8, NIH, Bethesda, MD, USA).

Enzyme-Linked Immunosorbent Assay (ELISA)

ATDC5 cells were treated with interleukin (IL)-1β (10 ng/mL) for 24 hours to mimic OA in vitro. Inflammatory cytokines and antioxidants, including IL-6, prostaglandin E2 (PGE2), tumor necrosis factor-alpha (TNF-α), malondialdehyde (MDA), glutathione (GSH), and superoxide dismutase (SOD), were detected in the supernatants using ELISA kits (Huding Biotechnology Co., Shanghai, China). The optical density at 450 nm was measured using a microplate reader (Epoch2, BioTek).

OA Model and Animal Treatment

The Laboratory Animal Management and Use Committee of the Hubei Provincial Center for Disease Control and Prevention approved the animal experiments (202410339). Thirty-two 8-week-old male C57BL/6 mice weighing 25 ± 2 g were purchased from Hubei Beinte Biotechnology Co., Ltd. The OA model was established in mice by destabilizing the medial meniscus (DMM) of the right knee joint, as previously described.[24] The mice were randomly divided into Sham, DMM model, DMM+AuNPs-miR-140, and DMM+Lipo-miR-140 groups, with eight mice per group. The animals were raised in separate cages and were allowed to move freely. Starting two weeks after the surgery, the mice received treatment-specific injection of 15 μL into the right knee joint via the medial parapatellar approach once every two weeks. Specifically, normal saline was injected into the Sham and DMM model control groups; AuNPs-miR-140 solution (containing 20 μg AuNPs and 2 μg miR-140-5p) into the DMM+AuNPs-miR-140 group; and Lipo-miR-140 solution (containing 2 μg miR-140-5p) into the DMM+Lipo-miR-140 group. After eight weeks, the mice were euthanized with CO_2, and their knee joint specimens were collected.

Specimen Preparation

The knee joints were fixed with 4% paraformaldehyde for 24 hours and decalcified with 14% ethylenediaminetetraacetic acid (EDTA) at room temperature for 5 weeks. Subsequently, the specimens were embedded in paraffin and cut longitudinally into 3-μm thick serial sections, sectioned laterally from the sagittal plane. The sections were labeled sequentially. Sections with the same label from each group were selected for histopathological and immunohistochemistry (IHC) analysis.

Histological Analysis

Some joint tissue sections were dewaxed, dehydrated, and stained with hematoxylin and eosin (H&E; C250201, Baso, Zhuhai, China) and safranin O-fast green (S&F; 20240407, Solarbio) to examine the structural integrity of the cartilage and underlying subchondral bone. Two investigators blinded to the experimental conditions used a light microscope (BX53, Olympus) to independently assess the tissue morphology. Cartilage degeneration was quantitatively analyzed according to standardized grading criteria established by the Osteoarthritis Research Society International (OARSI).[25]

Immunohistochemistry

IHC was conducted on 3-μm thick sagittal knee joint sections. The sections were deparaffinized using xylene and rehydrated through a graded ethanol series. Antigen retrieval was achieved via microwave heating for 20 minutes at 95°C in a pH 6.0 citrate-buffered solution. The sections were treated with 3% hydrogen peroxide (H_2O_2) for 15 minutes at room temperature to inhibit endogenous peroxidase activity. Non-specific binding was minimized by blocking the sections with 10% normal goat serum for one hour at room temperature. The sections were then incubated overnight at 4°C with primary antibodies targeting ACAN (1:200) and COL2 (1:300). After washes with phosphate-buffered saline (PBS), HRP-conjugated secondary antibodies were applied at a dilution of 1:500 for one hour at room temperature. The

staining intensity was quantified using ImageJ software by measuring the integrated density in the tibial plateau cartilage at 100× magnification for ACAN and COL2.

Statistical Analysis

The data are expressed as mean ± standard error of the mean (SEM) and were analyzed using GraphPad Prism (version 9.0, GraphPad Software, San Diego, CA, USA). The control and treatment groups were compared using a one-way analysis of variance (ANOVA), followed by Dunnett's post hoc test. Statistical significance was set at $p < 0.05$.

Results

Characterization of AuNPs and AuNPs-PEG-NH_2

The basic physicochemical characteristics of AuNPs and AuNPs-PEG-NH_2 are shown in Figure 1. They both had a spherical shape. The AuNPs diameter was 17.94 ± 5.51 nm when measured by FETEM (Figure 1A) and 26.05 ± 1.75 nm by dynamic light diameter (Figure 1B). The respective diameters of AuNPs-PEG-NH_2 were 18.70 ± 1.24 and 48.76 ± 1.95 nm (Figure 1A and Figure 1B). The polydispersity index (PDI) values for AuNPs and AuNPs-PEG-NH_2 were 0.16 ± 0.02 and 0.18 ± 0.01, respectively. Phase analysis light scattering (PALS) showed that the zeta potential of the AuNPs changed from –9.43 ± 1.40 mV to 15.22 ± 0.99 mV after PEG-NH_2 modification. Additionally, electrophoretic mobility changed from 0.73 to 1.19 μm·cm/(V·s), indicating successful PEG-NH_2 modification since protonation of the surface amino groups (NH_2) to NH_3^+ imparted a positive charge to the nanoparticles (Figure 1C). The ultraviolet-visible absorption spectrum of AuNPs and AuNPs-PEG-NH_2 showed a single peak at around 520 nm (Figure 1D). The aqueous solutions of AuNPs and AuNPs-PEG-NH2 are dark red (Figure 1E).

AuNPs-PEG-NH_2-Mediated miR-140 Delivery Efficiency

The Cy3 fluorescence intensity and the rate of Cy3-miR-140- positive cells in cells transfected with 10 μg/mL AuNPs and 40 nM Cy3-miR-140 for 24 hours were approximately 80 and 15 times higher, respectively, than in cells transfected with 40 nM Cy3-miR-140 alone. These findings indicate that AuNPs-PEG-NH_2 successfully delivered miR-140-5p into the cells (Figure 2A–D).

Effects of AuNPs-miR-140 on Chondrocyte Viability

After 48 hours of treatment, cell viability, assessed by the CCK-8 assay, showed no significant alterations at AuNPs concentrations of 0–40 μg/mL (corresponding to miR-140-5p concentrations of 0–80 nM; Figure 2E). These results indicate that AuNPs-miR-140 exhibited no detectable toxicity toward murine chondrocytes at the tested concentrations.

The Biological Function of AuNPs-miR-140 Complexes

The expression of miR-140-5p in the AuNPs-miR-140 complex-treated group was 5-fold higher than in the free miR-140-5p group. The mRNA expression levels of MMP-13 and ADAMTS5 significantly decreased, while those of COL2 and ACAN significantly increased in the AuNPs-miR-140 complex-treated group (Figure 3A).

Western blot analysis revealed a significant increase in the expression of MMP-13 and ADAMTS5, the two main cartilage matrix-degrading enzymes, after inducing inflammation with IL-1β. However, this effect was reversed when the cells were treated with AuNPs-miR-140 complexes (Figure 3B–F). In contrast, free miR-140-5p did not affect the expression of MMP-13 and ADAMTS5, indicating that exogenous miR-140-5p requires vector delivery to enter cells and exert its biological effects. The expression of COL2 and ACAN also increased significantly after treating the cells with AuNPs-miR-140 complexes.

ELISA results showed that the levels of pro-inflammatory cytokines (IL-6, PGE2, TNF-α) increased significantly in chondrocytes treated with IL-1β. These increases were significantly inhibited when the cells were treated with AuNPs-miR-140 complexes. Moreover, the AuNPs-miR-140 complexes exhibited an antioxidant effect by promoting the expression of SOD and GSH (Figure 3G).

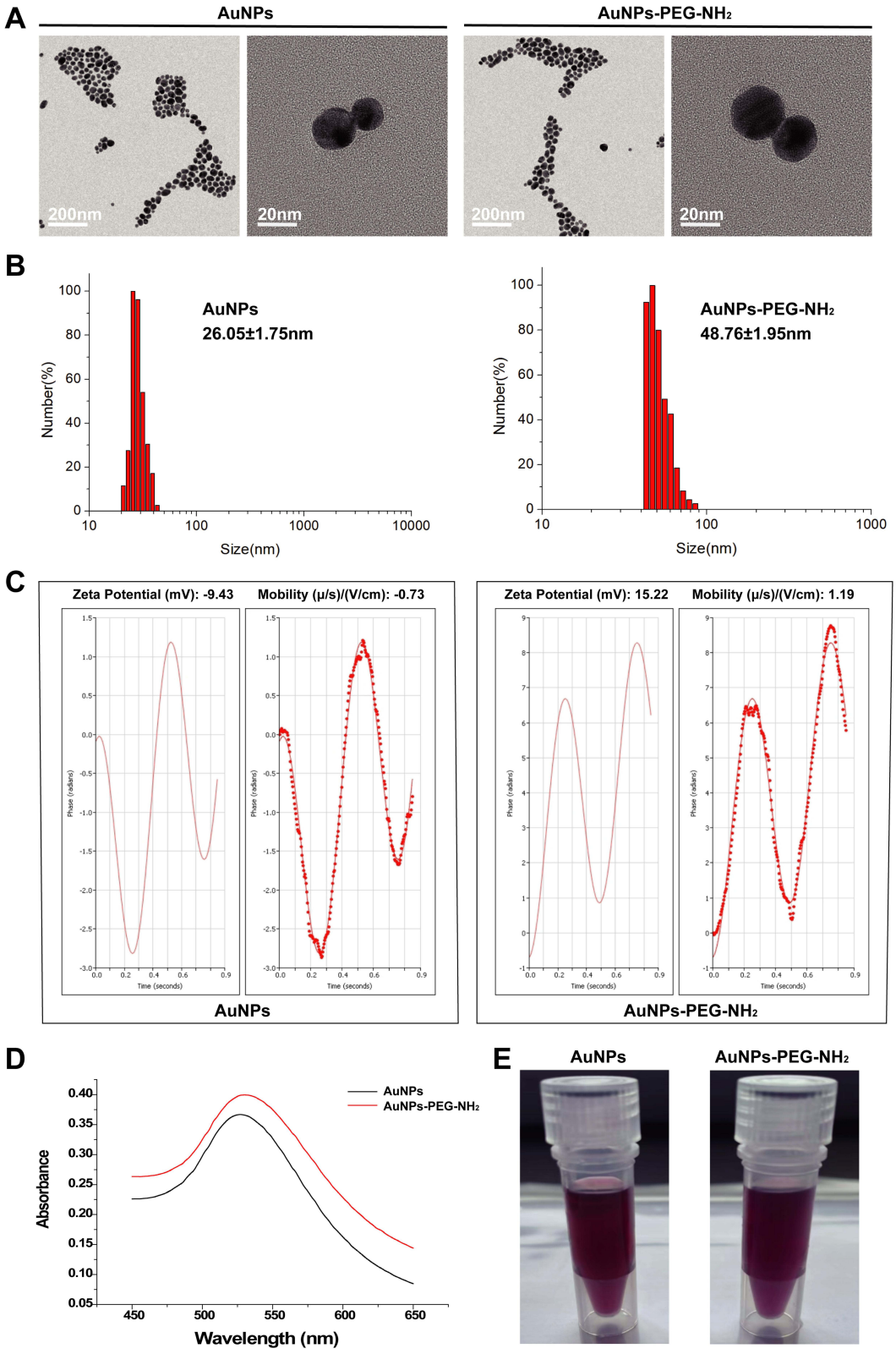

Figure 1 Characterization of gold nanoparticles (AuNPs) and polyethylene glycol-aminated AuNPs (AuNPs-PEG-NH_2). (**A**) Field emission transmission electron microscopy (FETEM) showed that AuNPs and AuNPs-PEG-NH_2 are spherical, with uniform size and distribution. (**B**) The dynamic light scattering diameters of AuNPs and AuNPs-PEG-NH_2 were 26.05 ± 1.75 and 48.76 ± 1.95 nm, respectively. (**C**) Phase analysis light scattering (PALS) showed that the zeta potential of AuNPs changed from –9.43 ± 1.40 mV to 15.22 ± 0.99 mV after PEG-NH_2 modification. The electrophoretic mobility changed from 0.73 to 1.19 μm·cm/(V·s). (**D**) The ultraviolet-visible absorption spectrum of AuNPs and AuNPs-PEG-NH_2 peaked at approximately 520 nm. (**E**) The aqueous solutions of AuNPs and AuNPs-PEG-NH_2 are dark red.

https://doi.org/10.2147/IJN.S585900

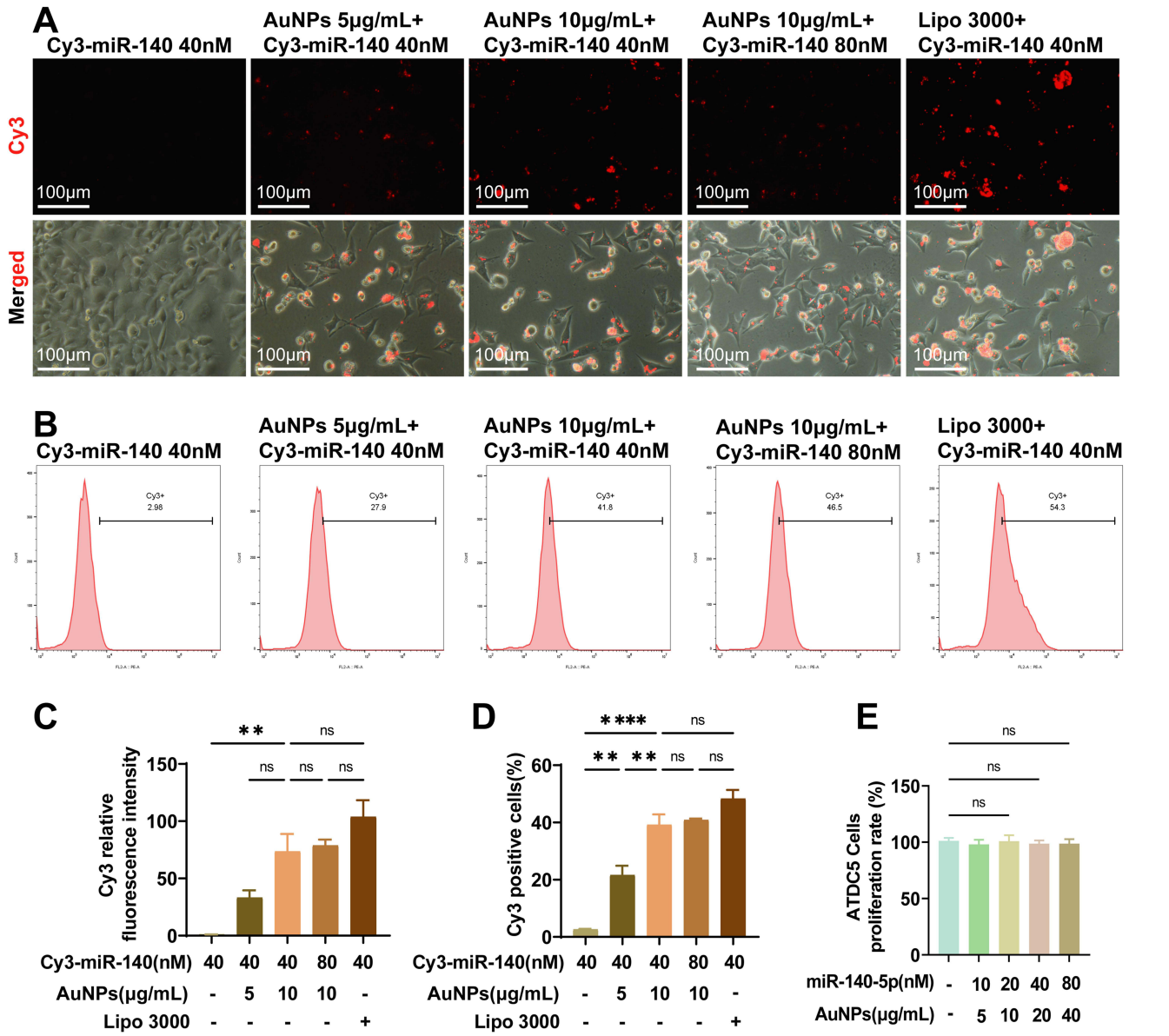

Figure 2 AuNPs-PEG-NH_2 mediates miR-140 delivery efficiency. (**A**) Fluorescence microscopy shows that the AuNPs-Cy3-miR-140 complexes were internalized by cells. (**B**) The Cy3-miR-140-positive cell rate detected by flow cytometry in the AuNPs groups was higher than in the free Cy3-miR-140 group. (**C**) Quantitative analysis of AuNPs-PEG-NH_2 delivery efficiency by fluorescence intensity detect. (**D**) Quantitative analysis of Cy3-miR-140-positive cell rate detected by flow cytometry. (**E**) AuNPs-miR-140 exhibited no detectable toxicity toward ATDC5 cells at the tested concentrations. The results are presented as mean ± SEM. $^{**}p < 0.01$; $^{****}p < 0.0001$; n = 3.

Kinetics of miR-140-5p Intracellular Release from the AuNPs-PEG-NH_2 Carriers

The kinetics of miR-140-5p intracellular release from the AuNPs-PEG-NH_2 carriers exhibited a marked time-dependent pattern. The free miR-140-5p and control groups exhibited comparable levels at all time points. Lipo 3000-encapsulated miR-140-5p displayed an initial burst release during the first two days, with gradual attenuation by day 7 and sustained low-level release until day 14. In contrast, the AuNP-miR-140 group showed superior sustained-release properties: the initial release during the first 12 hours was minimal; it was followed by progressively increased release rate during days 1–3 and reached a stable plateau by day 7, which was maintained through day 14. These findings indicate that the AuNP-PEG-NH_2 carrier system significantly enhanced the durability and stability of miRNA release. This effect is likely attributed to the protection of the surface modifications against enzymatic degradation and the slow-release mechanism

https://doi.org/10.2147/IJN.S585900

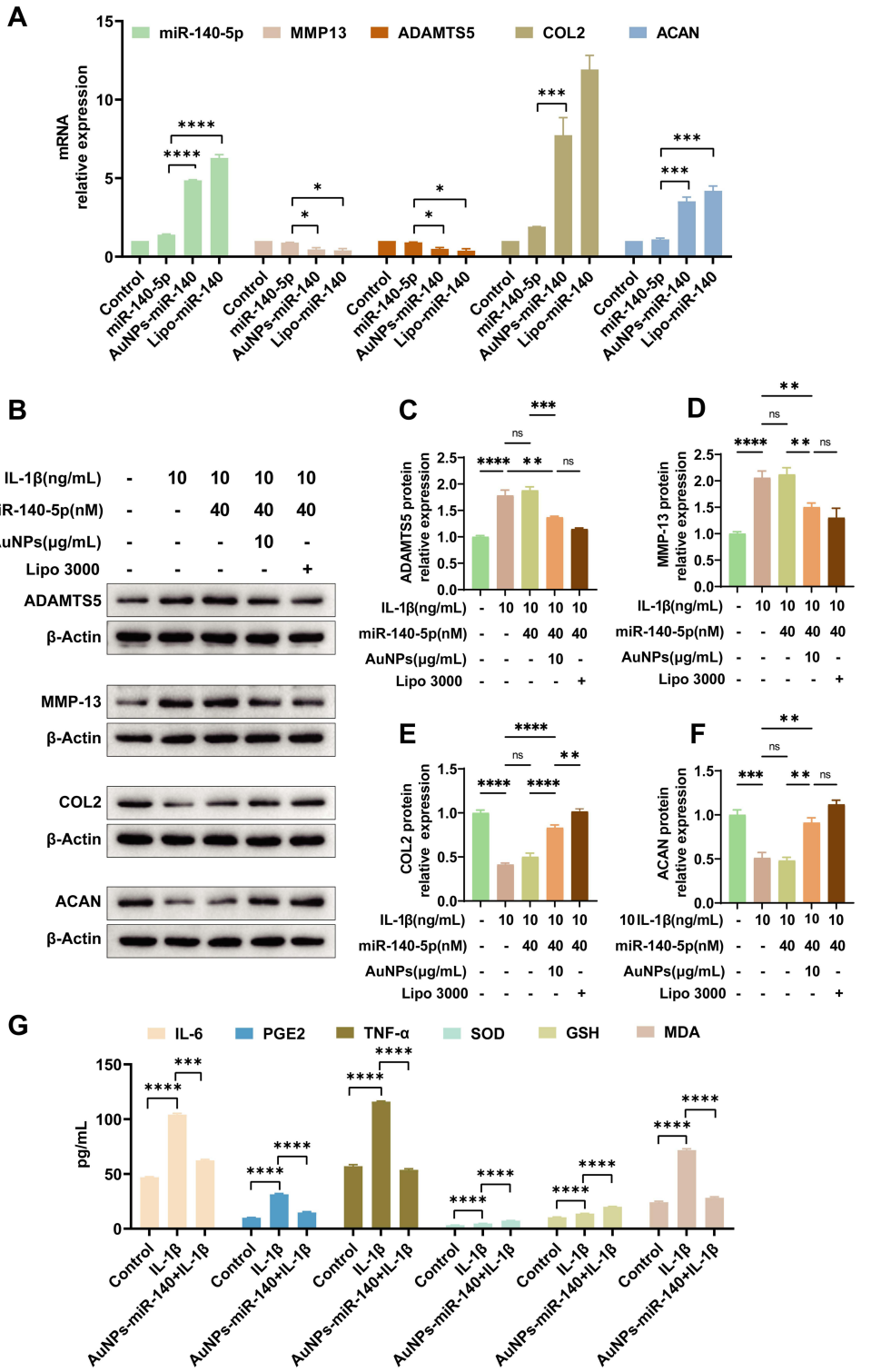

Figure 3 AuNPs-miR-140 complexes attenuate chondrocyte injury mediated by the inflammatory cytokine interleukin (IL)-1β. (**A**) The expression of miR-140-5p and MMP13 mRNA, ADAMTS5 mRNA, COL2 mRNA, and ACAN mRNA were detected by reverse transcription quantitative real-time polymerase chain reaction (RT-qPCR). (**B**) The protein levels of matrix metallopeptidase-13 (MMP-13), a disintegrin and metalloproteinase with thrombospondin motifs 5 (ADAMTS5), collagen II (COL2), and aggrecan (ACAN) were quantified by Western blot. (**C**) Quantification analysis result of ADAMTS5. (**D**) Quantification analysis result of MMP13. (**E**) Quantification analysis result of COL2. (**F**) Quantification analysis result of ACAN. *$p < 0.05$; **$p < 0.01$; ***$p < 0.001$; ****$p < 0.0001$. (**G**) The levels of pro-inflammatory cytokines and antioxidants were analyzed quantitatively by ELISA. The results are presented as mean ± SEM (n = 3).

https://doi.org/10.2147/IJN.S585900

after internalization by endocytosis. The distinct kinetic profile of this delivery system suggests that AuNPs-PEG-NH_2 is advantageous for long-term miRNA delivery applications (Figure 4A).

RT-qPCR detected a significant downregulation of miR-140-5p expression in the OA model groups (Figure 4B). The miR-140-5p level in chondrocytes of the saline-treated OA model group was approximately 90% lower than in the Sham group ($p < 0.001$). The miR-140-5p level in the chondrocytes was significantly restored after treatment with AuNPs-miR-140 (the DMM+AuNPs-miR-140 group) and was approximately three times higher than in the DMM model group ($p = 0.009$), but significantly lower than in the Sham group ($p < 0.001$). The miR-140-5p expression level in the DMM+AuNPs-miR-140 group was insignificantly lower than in the DMM+Lipo-miR-140 group ($p = 0.063$), possibly due to the small sample size.

The AuNPs-miR-140 Complexes Attenuate OA Progression in the DMM Mouse Model

Under dissecting microscopy, fresh macroscopic specimens revealed a loss of cartilage surface luster and erosions/pitting in the medial femoral condyle and medial tibial plateau in DMM-induced OA mice. Cartilage denudation was more severe in the DMM group than in the sham, DMM+AuNPs-miR-140, and DMM+Lipo-miR-140 group (Figure 4C).

The representative histomorphometric micrographs in Figure 4D demonstrate distinct morphological differences: The Sham group exhibited preserved articular architecture with intact cartilage surfaces, physiologically aligned chondrocyte populations, and physiological joint spacing. In contrast, the DMM model group displayed marked cartilage degradation, characterized by surface cartilage fibrillation and disrupted chondrocyte organization. Therapeutic intervention with AuNPs-miR-140 and Lipo-miR-140 significantly attenuated these degenerative changes, showing cartilage layer preservation. Complementary S&F staining corroborated these findings, demonstrating enhanced proteoglycan retention and homogeneous extracellular matrix distribution in the DMM+AuNPs-miR-140 group compared to DMM model group injected with saline (Figure 4E). The OARSI score in AuNPs-miR-140 group was significantly lower than that in the DMM control group ($p < 0.001$) (Figure 4F).

AuNPs-miR-140 Complexes Suppress Extracellular Matrix (ECM) Degradation in the DMM Model

To evaluate the therapeutic efficacy of AuNPs-miR-140 against extracellular matrix (ECM) degradation in OA, IHC analysis was performed on cartilage tissues from OA model mice. The IHC results demonstrated that the expression of anabolic markers (COL2 and ACAN) in DMM mice treated with AuNPs-miR-140 was notably upregulated compared with DMM mice treated saline (Figure 5A). Quantitative assessment of IHC-positive stained areas further corroborated the ECM-preserving capacity of this nanoformulation (Figures 5B).

Discussion

This study demonstrated that PEG-NH_2-modified AuNPs could serve as an efficient, biocompatible delivery platform for miR-140-5p to effectively alleviate OA progression by modulating cartilage matrix homeostasis and inhibiting inflammatory responses. The main findings of this study include: (1) AuNPs-PEG-NH_2 significantly enhanced the stability and uptake efficiency of miR-140-5p in chondrocytes; (2) AuNPs-miR-140 complexes inhibited key catabolic enzymes (MMP-13, ADAMTS5) and inflammatory mediators (IL-6, TNF-α), and promoted the synthesis of anabolic markers (COL2, ACAN); (3) injection of AuNPs-miR-140 into the joint cavity significantly attenuated cartilage degeneration in an OA mouse model, highlighting its therapeutic potential.

miR-140-5p exerted its therapeutic effects by targeting catabolism and inflammation in OA. The core mechanism behind its therapeutic effect involves regulating the expression of cartilage matrix-degrading enzymes, such as ADAMTS5 and MMP-13, which are directly involved in degrading extracellular matrix proteins, such as COL2 and ACAN.[6,26] RT-qPCR and Western blot data confirmed that AuNPs-miR-140 significantly downregulated MMP-13 and ADAMTS5 expression and upregulated the expression of COL2 and ACAN, consistent with the reported inhibition of the NF-κB pathway by miR-140.[8] Notably, the decrease in IL-6 and TNF-α levels suggested an indirect regulatory effect of miR-140-5p on synovial inflammation. Furthermore, SOD and GSH activities were enhanced in chondrocytes of the miR-140-5p-treated group, suggesting that

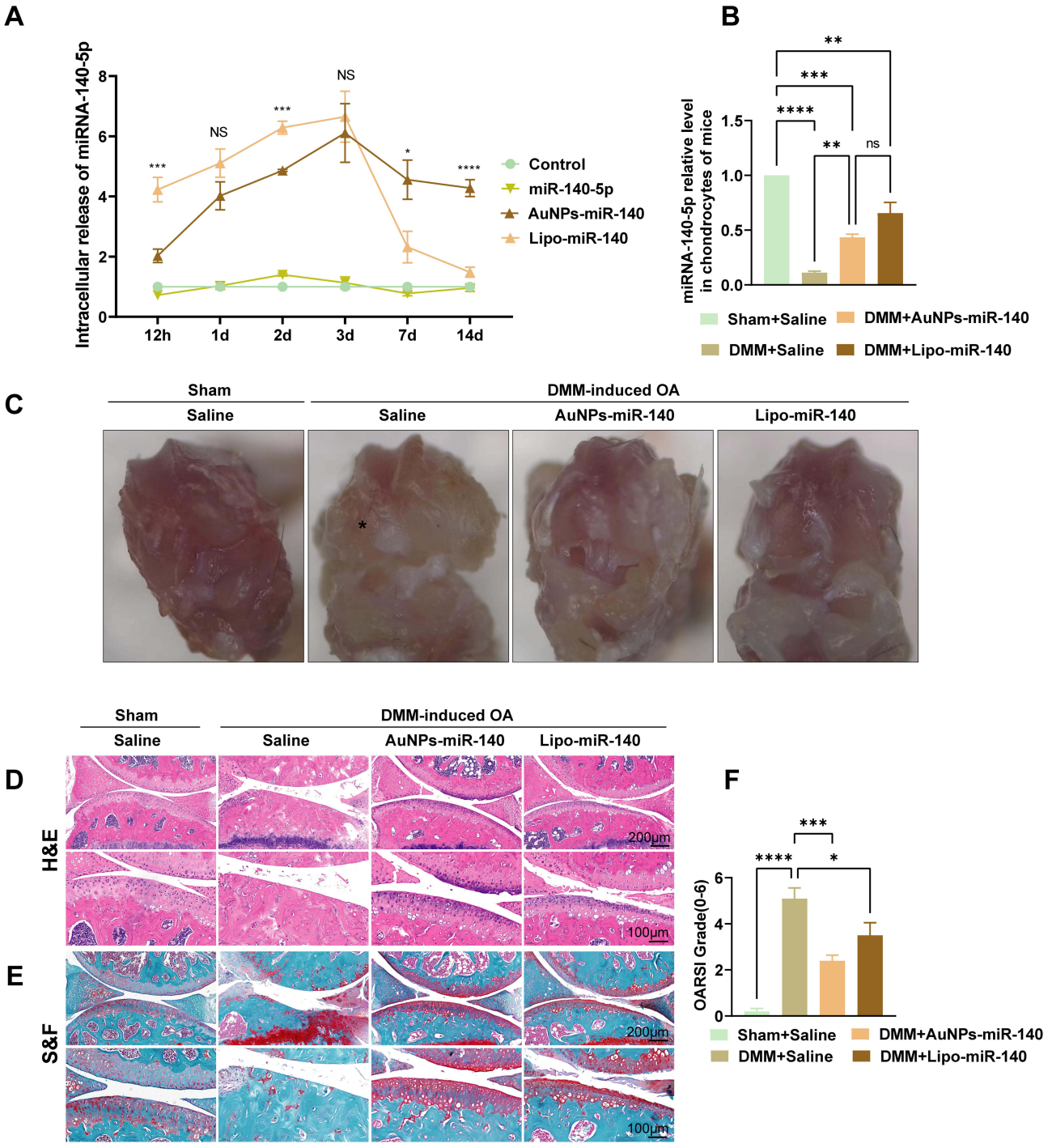

Figure 4 AuNPs-miR-140 complexes attenuate OA progression in the DMM mouse model. (**A**) RT-qPCR detected the intracellular release kinetics of miR-140-5p in vitro (*p < 0.05; ***p < 0.001; ****p < 0.0001; ns: non-significant. AuNPs-miR-140 vs. Lipo-miR-140 group). (**B**) RT-qPCR detected miR-140-5p relative levels in chondrocytes of mice eight weeks after the DMM operation. (**C**) Macroscopic appearance of fresh mouse knee joints under dissecting microscopy. The asterisk (*) indicates cartilage stripping of the medial femoral condyle. (**D**) Hematoxylin and eosin (H&E) staining were used to observe morphological variations in the articular cartilage. (**E**) Safranin O-fast green (S&F) staining displayed the variation of glycosamine polysaccharide in the articular cartilage. (**F**) The Osteoarthritis Research Society International (OARSI) scoring system evaluated the tibial plateau cartilage. The results are presented as mean ± SEM (n = 3 in A and B; n = 5 in F). *p < 0.05; **p < 0.01; ***p < 0.001; ****p < 0.0001.
Abbreviation: ns, non-significant.

miR-140-5p possesses an antioxidant function, antagonizing reactive oxygen species (ROS)-mediated matrix degradation. This multi-pathway effects endows miR-140-5p with a clinical advantage over single-target therapies, such as MMP inhibitors, which often show limited efficacy due to compensatory mechanisms.

https://doi.org/10.2147/IJN.S585900

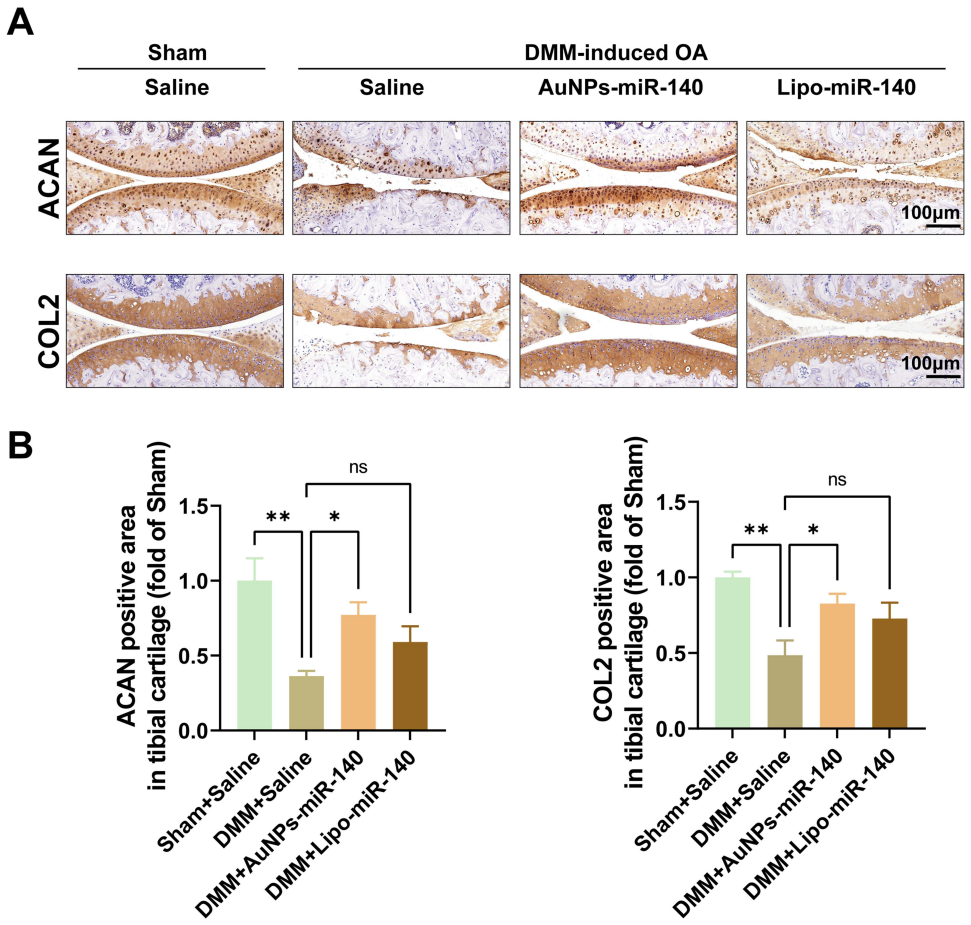

Figure 5 AuNPs-miR-140 complexes suppress extracellular matrix (ECM) degradation in the DMM mouse model. (**A**) Immunohistochemistry (IHC) demonstrated variation in COL2, and ACAN in cartilage tissue samples. (**B**) Quantification of cells positive for COL2 and ACAN in cartilage tissue samples. The results are presented as mean ± SEM (n = 5). *$p < 0.05$; **$p < 0.01$.
Abbreviation: ns, non-significant.

Although Si et al,[7] demonstrated that intra-articular injections of miR-140-5p slowed OA progression, the instability of free miRNAs in the synovial fluid remains an important therapeutic barrier, especially within this inflammatory microenvironment. Synovial fluid is rich in complex components, such as proteins, which can impair miRNA efficacy through degradation or chelation.[27] The in vitro experiments in this study showed that free miR-140-5p could not effectively regulate MMP-13 or ADAMTS5 expression, presumably due to enzymatic degradation and insufficient cellular uptake. In contrast, AuNPs-PEG-NH_2 protected miR-140-5p from nuclease degradation and achieved 15-fold higher cellular uptake. This result is consistent with reports that cationic nanoparticles (eg, PEI and lipid carriers) enhance nucleic acid stability through electrostatic interactions[28,29] Given its positive surface charge (+15.22 mV), AuNPs-PEG-NH_2 effectively binds negatively charged miRNAs.

The modification strategy employed aimed to simultaneously enhance nanoparticle stability, biocompatibility, and cellular uptake efficiency. The PEGylated modification can help avoid trapping by the reticuloendothelial system and prolong blood circulation time,[30,31] ensuring that a sufficient quantity of nanoparticles can reach the target cells to exert therapeutic effects. The surface amino group (NH_2) enables cartilage-targeted ligand coupling and binds negatively charged nucleic acids, such as miR-140, through electrostatic interaction, guaranteeing chondrocyte-specific delivery.[32] This delivery system exhibits unique advantages over cationic liposomes, which, despite high transfection efficiency, are prone to cytotoxicity and immunogenicity due to their cationic nature,[33] and exhibit a short circulation time due to aggregation in the presence of serum proteins.[34]

PEG-modified nanoparticles also offer the advantage of a slow-release effect, a particularly important property in OA therapy. The management of chronic inflammation and joint damage requires the sustained release of therapeutic agents. Studies systematically describe the use of polymer colloids as a drug delivery system for arthritis,[35] emphasizing the importance of maintaining long-term effective therapeutic concentrations through controlled drug release. This approach is highly compatible with the slow-release advantages of PEGylated nanoparticles. Our in vitro experiments confirmed that AuNPs-PEG-NH_2 exhibited excellent stability and slow-release properties. High intracellular miR-140-5p levels were detected even after 14 days of cell culture, demonstrating the long-acting, sustained-release ability of this vector, making it an ideal delivery system for chronic OA treatment. This slow-release profile of AuNPs-PEG-NH_2 was significantly better than that of the Lipo vector, which decreased to near-basal levels by day 7. The in vivo results further confirmed that injection of AuNPs-miR-140 into the joint cavity effectively inhibited OA progression, demonstrating promising therapeutic prospects.

Although research on AuNP-based miRNA delivery for OA is limited, existing studies support the rationale for our AuNPs-PEG-NH_2 carrier. Ren et al[36] showed that PAMAM-functionalized hollow AuNPs encapsulate miRNAs inhibitors and drugs via cationic interactions, with the gold shell protecting against nuclease degradation. Sukumar et al[37] demonstrated that gold-iron oxide hybrid nanoparticles with a β-cyclodextrin-chitosan coating bind therapeutic miRNAs electrostatically, protect them from ribonuclease, and enable effective in vivo delivery and gene silencing. A 2024 study on poly(β-amino-ester)-coated gold nanocages confirmed that cationically modified AuNPs protect siRNA from nucleases, enhance chondrocyte uptake, and prolong drug retention in joints through charge-mediated cartilage anchoring.[38] Collectively, these findings confirm that cationically modified AuNPs can bind miRNAs, resist nuclease degradation, improve cellular uptake, and achieve effective in vivo delivery, providing strong support for our PEG-NH_2-modified AuNPs as miRNA carrier.

Despite the positive results of the in vivo experiments in this study, as demonstrated by a reduction in OARSI score and preservation of cartilage integrity, some translational medicine challenges should be considered: First, the short-term efficacy assessment in the mouse model (eight weeks) may be insufficient to predict the long-term therapeutic efficacy in chronic human OA; second, due to the lack of active targeting ligands, such as CD44, integrin-binding peptide, the specificity of our system for chondrocytes is limited, increasing the risk of off-targeting during clinical application. Recent studies have shown that hyaluronic acid-coupled nanoparticles can significantly enhance the efficiency of cartilage retention and cell-specific delivery,[39] suggesting a direction for optimizing AuNPs-PEG-NH_2; third, the DMM surgically induced inflammatory OA model mainly mimics post-traumatic OA, whereas age-associated or metabolic OA subtypes may require the development of individualized treatment strategies.

To promote the clinical translation of AuNPs-miR-140, subsequent studies should focus on the following directions: (1) developing a targeted delivery system modified with cartilage-homing ligands, such as a Col II-binding peptide, to enhance the enrichment of nanoparticles in degenerative joints; (2) constructing a co-delivery system of miR-140-5p with anti-inflammatory agents, such as curcumin or IL-1Ra, to enhance efficacy through synergistic modulation of catabolic and inflammatory pathways;[40] (3) carrying out long-term safety assessment in large animals and systematically investigate the distribution, immune response, and off-target effects of the nanocomplexes, aiming to determine the feasibility of clinical translation.

Conclusion

In conclusion, we report for the first time a PEG-NH_2-modified gold nanoparticle platform for delivering miR-140-5p to treat OA. The constructed AuNPs-PEG-NH_2 system delivers miR-140-5p with a 15-fold higher uptake by chondrocytes and achieves sustained release for up to 14 days in vitro, representing an efficient intra-articular miRNA delivery platform that successfully overcomes the critical limitations of free miRNA therapy. This system effectively restored cartilage homeostasis and delayed OA progression by enhancing miR-140-5p bioactivity and promoting chondrocyte uptake. Future studies should advance the clinical application of this technology by integrating targeted modifications and combinatorial therapeutic strategies, thus offering new hope for developing OA therapies with disease-modifying effects.

https://doi.org/10.2147/IJN.S585900

Abbreviations

ACAN, Aggrecan; ADAMTS5, a disintegrin and metalloproteinase with thrombospondin motifs 5; ANOVA, analysis of variance; AuNPs, gold nanoparticles; BSA, bovine serum albumin; COL2, collagen II; DMEM/F-12, Dulbecco's Modified Eagle's Medium/Nutrient Mixture F-12; DMM, destabilizing the medial meniscus; EDTA, ethylenediaminetetraacetic acid; ELISA, enzyme-linked immunosorbent assay; FBS, fetal bovine serum; GSH, glutathione; H&E, hematoxylin and eosin; HRP, horseradish peroxidase; IHC, immunohistochemistry; IL, interleukin; MDA, malondialdehyde; miR-140, microRNA-140; MMP, matrix metalloproteinase; NF-κB, nuclear factor κB; OA, osteoarthritis; OARSI, Osteoarthritis Research Society International; OD, optical density; PALS, phase analysis light scattering; PBS, phosphate-buffered saline; PDI, polydispersity index; PEG, polyethylene glycol; PEI, polyethyleneimine; PGE2, prostaglandin E2; PMSF, phenylmethylsulphonyl fluoride; RIPA, radioimmunoprecipitation assay; ROS, reactive oxygen species; S&F, safranin O-fast green; SEM, standard error of the mean; SOD, superoxide dismutase; TBST, tris-buffered saline Tween; TNF-α, tumor necrosis factor-alpha.

Data Sharing Statement

All data generated or analyzed during this study are available from the corresponding author, Xiangping Luo, upon reasonable request.

Ethics Approval

The Laboratory Animal Management and Use Committee of the Hubei Provincial Center for Disease Control and Prevention approved the animal experiments (202410339) and conducted in accordance with the NIH Guide for the Care and Use of Laboratory Animals. The manuscript confirming the study is reported in accordance with ARRIVE guidelines.

Acknowledgments

We appreciate the experimental technical assistance provided by Keyi Biotechnology (Wuhan) Co., Ltd.

Author Contributions

All authors made a significant contribution to the work reported, whether that is in the conception, study design, execution, acquisition of data, analysis and interpretation, or in all these areas; took part in drafting, revising or critically reviewing the article; gave final approval of the version to be published; have agreed on the journal to which the article has been submitted; and agree to be accountable for all aspects of the work.

Funding

This study was funded by Hunan Provincial Natural Science Foundation (No.2023JJ50098).

Disclosure

The author(s) report no conflicts of interest in this work.

References

1. Glyn-Jones S, Palmer AJR, Agricola R, et al. Osteoarthritis. *Lancet*. 2015;386(9991):376–387. doi:10.1016/S0140-6736(14)60802-3
2. Berenbaum F. Osteoarthritis as an inflammatory disease (osteoarthritis is not osteoarthrosis!). *Osteoarthritis Cartilage*. 2013;21(1):16–21. doi:10.1016/j.joca.2012.11.012
3. G SM, Beier F, A PM. Recent developments in emerging therapeutic targets of osteoarthritis. *Curr Opin Rheumatol*. 2017;29(1):96–102. doi:10.1097/BOR.0000000000000351
4. Grol MW. The evolving landscape of gene therapy strategies for the treatment of osteoarthritis. *Osteoarthritis Cartilage*. 2024;32(4):372–384. doi:10.1016/j.joca.2023.12.009
5. Evans CH, Ghivizzani SC, Robbins PD. Osteoarthritis gene therapy in 2022. *Curr Opin Rheumatol*. 2023;35(1):37–43. doi:10.1097/BOR.0000000000000918
6. Zhang Y, Lin J, Zhou X, et al. Melatonin prevents osteoarthritis-induced cartilage degradation via targeting MicroRNA-140. *Oxid Med Cell Longev*. 2019;14:9705929.

7. Si HB, Zeng Y, Liu SY, et al. Intra-articular injection of microRNA-140 (miRNA-140) alleviates osteoarthritis (OA) progression by modulating extracellular matrix (ECM) homeostasis in rats. *Osteoarthritis Cartilage*. 2017;25(10):1698–1707. doi:10.1016/j.joca.2017.06.002
8. Karlsen TA, de Souza GA, Ødegaard B, Engebretsen L, Brinchmann JE. microRNA-140 inhibits inflammation and stimulates chondrogenesis in a model of interleukin 1β-induced osteoarthritis. *Mol Ther Nucleic Acids*. 2016;5(10):e373. doi:10.1038/mtna.2016.64
9. Al-Modawi RN, Brinchmann JE, Karlsen TA. Multi-pathway protective effects of micrornas on human chondrocytes in an in vitro model of osteoarthritis. *Mol Ther Nucleic Acids*. 2019;17:776–790. doi:10.1016/j.omtn.2019.07.011
10. Cao F, Chen Y, Wang X, et al. Therapeutic effect and potential mechanisms of intra-articular injections of miR-140-5p on early-stage osteoarthritis in rats. *Int Immunopharmacol*. 2021;96:107786. doi:10.1016/j.intimp.2021.107786
11. Lee HP, Gu L, Mooney DJ, Levenston ME, Chaudhuri O. Mechanical confinement regulates cartilage matrix formation by chondrocytes. *Nat Mater*. 2017;16(12):1243–1251. doi:10.1038/nmat4993
12. Rahimi M, Charmi G, Matyjaszewski K, Banquy X, Pietrasik J. Recent developments in natural and synthetic polymeric drug delivery systems used for the treatment of osteoarthritis. *Acta Biomater*. 2021;123:31–50. doi:10.1016/j.actbio.2021.01.003
13. Mehryab F, Rabbani S, Shahhosseini S, et al. Exosomes as a next-generation drug delivery system: an update on drug loading approaches, characterization, and clinical application challenges. *Acta Biomater*. 2020;113:42–62. doi:10.1016/j.actbio.2020.06.036
14. Dalle Carbonare L, Bertacco J, Gaglio SC, et al. Fisetin: an integrated approach to identify a strategy promoting osteogenesis. *Front Pharmacol*. 2022;13:890693. doi:10.3389/fphar.2022.890693
15. Jin M, Jin G, Kang L, Chen L, Gao Z, Huang W. Smart polymeric nanoparticles with pH-responsive and PEG-detachable properties for co-delivering paclitaxel and survivin siRNA to enhance antitumor outcomes. *Int J Nanomed*. 2018;13:2405–2426. doi:10.2147/IJN.S161426
16. Zhu J, Yang S, Qi Y, et al. Stem cell-homing hydrogel-based miR-29b-5p delivery promotes cartilage regeneration by suppressing senescence in an osteoarthritis rat model. *Sci Adv*. 2022;8(13):eabk0011. doi:10.1126/sciadv.abk0011
17. Chen M, Lu Y, Liu Y, et al. injectable microgels with hybrid exosomes of chondrocyte-targeted fgf18 gene-editing and self-renewable lubrication for osteoarthritis therapy. *Adv Mater*. 2024;36(16):e2312559. doi:10.1002/adma.202312559
18. Ding Y, Jiang Z, Saha K, et al. Gold nanoparticles for nucleic acid delivery. *Mol Ther*. 2014;22(6):1075–1083. doi:10.1038/mt.2014.30
19. Huang PT, Chen YL, Lin YH, Wang CC, Chang HT. Functional gold nanoparticles for analysis and delivery of nucleic acids. *J Food Drug Anal*. 2024;32(3):252–273. doi:10.38212/2224-6614.3514
20. Okła E, Białecki P, Kędzierska M, et al. Pegylated gold nanoparticles conjugated with siRNA: complexes formation and cytotoxicity. *Int J Mol Sci*. 2023;24(7):6638. doi:10.3390/ijms24076638
21. Li X, Dai B, Guo J, et al. Nanoparticle-cartilage interaction: pathology-based intra-articular drug delivery for osteoarthritis therapy. *Nanomicro Lett*. 2021;13(1):149. doi:10.1007/s40820-021-00670-y
22. Li H, Pan S, Xia P, et al. Advances in the application of gold nanoparticles in bone tissue engineering. *J Biol Eng*. 2020;14:14. doi:10.1186/s13036-020-00236-3
23. Turkevich J, Stevenson PC, Hillier J. A study of the nucleation and growth processes in the synthesis of colloidal gold. *Discuss Faraday Soc*. 1951;11:55–75. doi:10.1039/df9511100055
24. Glasson SS, Blanchet TJ, Morris EA. The surgical destabilization of the medial meniscus (DMM) model of osteoarthritis in the 129/SvEv mouse. *Osteoarthritis Cartilage*. 2007;15:1061–1069. doi:10.1016/j.joca.2007.03.006
25. Glasson SS, Chambers MG, Van Den Berg WB, Little CB. The OARSI histopathology initiative–recommendations for histological assessments of osteoarthritis in the mouse. *Osteoarthritis Cartilage*. 2010;18 Suppl 3:S17–23. doi:10.1016/j.joca.2010.05.025
26. Miyaki S, Sato T, Inoue A, et al. MicroRNA-140 plays dual roles in both cartilage development and homeostasis. *Genes Dev*. 2010;24 (11):1173–1185. doi:10.1101/gad.1915510
27. Mahendran SM, Oikonomopoulou K, Diamandis EP, Chandran V. Synovial fluid proteomics in the pursuit of arthritis mediators: an evolving field of novel biomarker discovery. *Crit Rev Clin Lab Sci*. 2017;54(7–8):495–505. doi:10.1080/10408363.2017.1408561
28. Montaño-González PA, Bravo-Lozano LM, Chevance S, et al. Interactions between PEI and biological polyanions and the ability of glycosaminoglycans in destabilizing PEI/peGFP-C3 polyplexes for genetic material release. *Int J Biol Macromol*. 2025;301:140351. doi:10.1016/j.ijbiomac.2025.140351
29. Ayad C, Libeau P, Lacroix-Gimon C, Ladavière C, Verrier B. LipoParticles: lipid-Coated PLA nanoparticles enhanced in vitro mRNA transfection compared to liposomes. *Pharmaceutics*. 2021;13(3):377. doi:10.3390/pharmaceutics13030377
30. Karim ME, Chowdhury EH. PEGylated strontium sulfite nanoparticles with spontaneously formed surface-embedded protein Corona restrict off-target distribution and accelerate breast tumour-selective delivery of siRNA. *J Funct Biomater*. 2022;13(4):211. doi:10.3390/jfb13040211
31. Jahangirian H, Kalantari K, Izadiyan Z, Rafiee-Moghaddam R, Shameli K, Webster TJ. A review of small molecules and drug delivery applications using gold and iron nanoparticles. *Int J Nanomed*. 2019;14:1633–1657. doi:10.2147/IJN.S184723
32. Nam J, Won N, Bang J, et al. Surface engineering of inorganic nanoparticles for imaging and therapy. *Adv Drug Deliv Rev*. 2013;65(5):622–648. doi:10.1016/j.addr.2012.08.015
33. Wei X, Shao B, He Z, et al. Cationic nanocarriers induce cell necrosis through impairment of Na(+)/K(+)-ATPase and cause subsequent inflammatory response. *Cell Res*. 2015;25(2):237–253. doi:10.1038/cr.2015.9
34. Zhao W, Zhuang S, Qi XR. Comparative study of the in vitro and in vivo characteristics of cationic and neutral liposomes. *Int J Nanomed*. 2011;6:3087–3098. doi:10.2147/IJN.S25399
35. Saeedi T, Alotaibi HF, Prokopovich P. Polymer colloids as drug delivery systems for the treatment of arthritis. *Adv Colloid Interface Sci*. 2020;285:102273. doi:10.1016/j.cis.2020.102273
36. Ren Y, Wang R, Gao L, et al. Sequential co-delivery of miR-21 inhibitor followed by burst release doxorubicin using NIR-responsive hollow gold nanoparticle to enhance anticancer efficacy. *J Control Release*. 2016;228:74–86. doi:10.1016/j.jconrel.2016.03.008
37. Sukumar UK, Bose RJC, Malhotra M, et al. Intranasal delivery of targeted polyfunctional gold-iron oxide nanoparticles loaded with therapeutic microRNAs for combined theranostic multimodality imaging and presensitization of glioblastoma to temozolomide. *Biomaterials*. 2019;218:119342. doi:10.1016/j.biomaterials.2019.119342
38. Qiao L, Li Z, Li B, et al. Combination of anti-inflammatory therapy and RNA interference by light-inducible hybrid nanomedicine for osteoarthritis treatment. *Acta Pharm Sin B*. 2024;14(11):5008–5025. doi:10.1016/j.apsb.2024.06.009

39. Zerrillo L, Gigliobianco MR, D'Atri D, et al. PLGA nanoparticles grafted with hyaluronic acid to improve site-specificity and drug dose delivery in osteoarthritis nanotherapy. *Nanomaterials*. 2022;12(13):2248. doi:10.3390/nano12132248
40. Papathanasiou I, Balis C, Trachana V, Mourmoura E, Tsezou A. The synergistic function of miR-140-5p and miR-146a on TLR4-mediated cytokine secretion in osteoarthritic chondrocytes. *Biochem Biophys Res Commun*. 2020;522(3):783–791. doi:10.1016/j.bbrc.2019.11.168